Angewandte Chemie
Eine Zeitschrift der Gesellschaft Deutscher Chemiker

Supporting Information

69451 Weinheim, Germany

Supporting Information for "Facile Oxy-Functionalization of Electron-Rich Metal Alkyl with OsO_4"

Brian L. Conley,[‡] Somesh K. Ganesh,[‡] Jason Gonzales,[†] Daniel H. Ess,[a†] Robert J. Nielsen,[†] Vadim R. Ziatdinov,[‡] Jonas Oxgaard,[†] William A. Goddard, III,[†]* and Roy A. Periana[a] *

[a]The Scripps Research Institute, Scripps Florida
5353 Parkside Drive, Jupiter, FL 33458
[‡]Donald P. and Katherine B. Loker Hydrocarbon Research Institute and Department of Chemistry, University of Southern California, Los Angeles, California 90089
[†]Materials and Process Simulation Center, Beckman Institute, Division of Chemistry and Chemical Engineering, California Institute of Technology, Pasadena, California 91125.

General Considerations: All air and water sensitive procedures were carried out either in a MBraun inert atmosphere glove box under N_2, or using standard Schlenk techniques under argon. Labeled reagents D_2O, $H_2{}^{18}O$ (Cambridge Isotopes) and KOD solution (40% wt. 98+ atom % D, Sigma-Aldrich) were used as purchased. Water, D_2O, and KOD were degassed by thoroughly purging with dry argon gas. Methyltrioxorhenium was purchased from Strem. OsO_4 was purchased from Pressure Chemical. Na_3PO_4 was purchased from J.T. Baker Chemical Company, Na_2HPO_4 from Mallinckrodt, and KH_2PO_4 from EMD. Sodium isonicotinate was purchased from TCI America. Extra dry grade oxygen used was purchased from Gilmore. GC/MS analysis was performed on a Shimadzu GC-MS QP5000 (ver. 2) equipped with cross-linked methyl silicone gum capillary column (DB5). The retention times of the products were confirmed by comparison to authentic samples. NMR spectra were obtained on a Varian Mercury-400 MHz spectrometer at room temperature. All chemical shifts are reported in units of ppm and referenced to the residual protonated solvent. Standard C,H,N elemental analysis was performed by Desert Analytics Laboratory in Tucson, AZ.

Procedure for Reaction of OsO_4 and MTO: Appropriate quantities of OsO_4 were weighed in a well ventilated fume hood, taking extra precaution with regard to sash level and air flow setting due to the unusual volatility and toxicity of the compound. Due to its volatility, osmium tetroxide is sticky and hard to manage at room temperature, but can easily be handled by dropping the glass vial in which it is stored into liquid nitrogen for a short time just prior to weighing, or by cooling inside the glove box freezer. The OsO_4 was dissolved in 0.5 mL D_2O followed by addition of KOD to form hydroxylated OsO_4 *in situ.* Methyltrioxorhenium was weighed out and dissolved in 0.5mL D_2O inside a Teflon fitted J-Young tube and sonicated and/or shaken until fully dissolved. Typical quantities that easily dissolve are between 10-15mg. The ^1H NMR of MTO and D_2O was first taken with a benzene/CCl_4 co-axial external standard. The oxidant solution was then added, the valve was sealed and the tube was inverted several times to mix the solutions. The ^1H NMR was then taken again. Integration of the methanol peak was multiplied by 2 to account for dilution and yields were calculated.

Pressurization with O_2: An MTO solution in D_2O was prepared as above. The ^1H NMR was taken after which the solution was transferred to a small (~0.75 mL) vial, which was made by sealing a glass pipet. A stainless steel, 5mL (total volume) Swagelok reactor was filled with oxidant solution as prepared above. The small vial was carefully set in the reactor (thus keeping the solutions partitioned) and the reactor was subsequently sealed. It was pressurized to 180 psi (12.2 atm) using Swagelok fittings and valve connected to the oxygen tank. After 5 minutes, the reactor was inverted and shaken to mix the two solutions. After mixing the reactor was opened and the resultant solution was transferred to the same NMR tube with co-axial standard. As reported in this communication, yields and selectivity to methanol of this reaction and of a similarly run control reaction (with no oxygen added) were statistically identical.

^{18}O-labeling Experiment: 15.0 mg of OsO_4 was dissolved in 0.25mL $H_2{}^{18}O$. Percent incorporation was determined by GC/MS analysis of the resulting solution immediately. OsO_4 elutes at ~3.4 minutes on the DB-5 column and has the following fragmentation patter: m/z 256 (100%), m/z 254 (64.4%), m/z 253 (39.6%), m/z 252 (32.5%), m/z 251 (4.8%), m/z 250 (3.9%). Since the predominant fragments in the spectrum are due to Os isotopes, the fragmentation pattern for $Os^{18}O_4$ (fully enriched) should simply be shifted by 8 mass units (i.e. at full incorporation m/z 264 would be the 100% peak). Thus, we deconvoluted by setting all the fragments in the MS spectrum relative to a 100% peak at m/z 264, subtracted all of the theoretical values (so for the m/z 264 peak 100%-100%, m/z 262 100%-64.4%, m/z 260 63.0%-32.5%, etc.). This removes all intensity for the fully incorporated molecule. We set the moles of OsO_4 equal to 1. The new value for the m/z 262 peak is 35.6% and thus we have a 1.0:0.356 ratio of $Os^{18}O_4$ to $Os^{18}O_3{}^{16}O$. We similarly deconvolute the whole spectrum to get the following values:

isotope	$Os^{18}O_4$	$Os^{18}O_3{}^{16}O$	$Os^{18}O_2{}^{16}O_2$	$Os^{18}O^{16}O_3$	$Os^{16}O_4$
mol isotope	1.000	0.356	0.214	0	0

To get the total moles of incorporated ^{18}O, we multiplied the moles of isotope by the corresponding number of oxygens (i.e. $Os^{18}O_3{}^{16}O$ has 1.068 moles of ^{18}O and 0.356 moles of ^{16}O). The total number of moles of oxygen was 6.28, 5.496 of which were ^{18}O for a total incorporation of 87%.

This solution was mixed with a 0.25 mL solution of 15.0mg MTO and 0.01 mL 40 % KOH in $H_2{}^{18}O$. The methanol produced from this reaction was labeled to ~95% ^{18}O as determined by GC/MS analysis. Methanol elutes simultaneously with water. We "find" the methanol by multiplying the m/z 32 or 34 GC trace by 1,000-10,000, then selecting the middle of that peak to look for relevant MS data. We compare the relative ratios of m/z 34 to m/z 32 for incorporation analysis.

A complementary experiment used the same amount of reagents, but MTO was dissolved in $H_2{}^{16}O$ before addition to the $Os^{18}O_{4-n}{}^{16}O_n$ solution. The product contained a 50:50 mixture of $CH_3{}^{16}OH$ to $CH_3{}^{18}OH$. Since we know that the incorporation of ^{18}O into MTO is slow on the time scale of the reaction, we are confident that the label in the product does not come from an oxygen on the Re starting material. The observed product ratio from this experiment suggests that oxygen can wash back into OsO_4 faster than the reaction to form methanol occurs.

Reaction of MTO and OsO_4/Isonicotinate: 0.5 mL of a 10mM MTO in D_2O solution was treated with 0.5mL of a 100mM OsO_4 solution containing 28.5 mg sodium isonicotinate. The following NMR spectra are typical for this experiment.

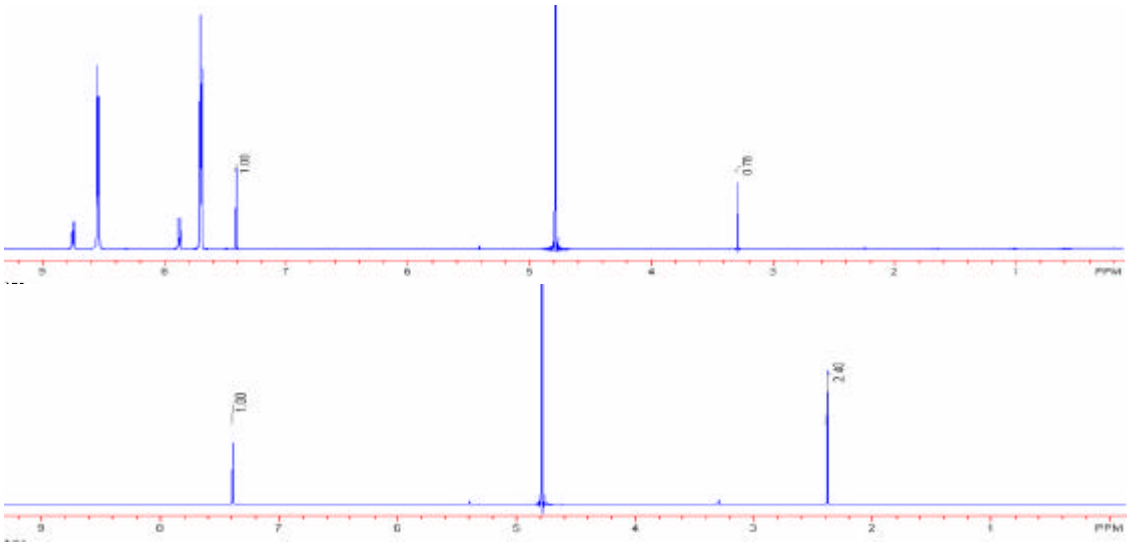

Figure S1. 400MHz ^1H NMR of MTO in D_2O with benzene/CCl_4 co-axial internal standard (bottom) and MTO in D_2O with added isonicotinic acid/OsO_4 solution (top). The peak at ~ d 3.3 is CH_3OH.

Buffered Experiments: Phosphate buffers were prepared in D_2O using Na_3PO_4, Na_2HPO_4, and KH_2PO_4 followed by adjustment of pH using a 40% KOD in D_2O solution.

Attempted Isolation of Methoxide Intermediate: In attempting to isolate a methoxide intermediate by trapping, MTO was reacted with OsO_4 in neat pyridine. Our intent was to provide an activating, non-protic media which we had previously demonstrated useful for the reaction of other O-atom donors.[1] The original solution became yellow-orange upon addition of equimolar amounts of MTO and OsO_4. Over the course of 24 h, the solution gradually turned darker, the resultant solution a deep forest green. After removal of solvent by reducing the pressure (~100mTorr) on a vacuum manifold, we were able to isolate the green solid and analyze it by NMR spectroscopy (^1H, ^{13}C NMR, elemental analysis, and infrared). This material was fairly difficult to manipulate, remaining sticky, probably due to an association with pyridine solvent molecules despite drying for days under reduced pressure. Attempts to wash with solvents such as ethanol and THF were deleterious to the green compound, resulting in dark black insoluble species and yellow-orange colored solutions. ^1H NMR and ^{13}C spectra were obtained in py-d_5, the only NMR solvent in which the compound was soluble (Figures S3 and S4). The proton NMR is consistent with the sticky nature of the compound, as free pyridine-*h5* is seen in solution upon dissolution in pyridine-*d5*. Three more equivalents of bound, protiated

pyridine can be accounted for based on the integration of the aromatic region, shown in Figure S3. The 2:1 ratio of peaks at d 9.11, d 8.86, d 7.19 vs. d 7.92, d 7.50, d 7.45 indicates that two of the bound pyridine molecules are symmetrical. Over time these resonances decay and the free pyridine resonances increase as the bound molecules exchange with the deuterated solvent. We believe that the peaks at d 6.16 and d 6.28 account for the methyl originally associated with MTO. Consistently, the intensity of these peaks does not change over the same time period necessary for complete pyridyl exchange. The methyl peak of the known pyridyl adduct of MTO shows up much further upfield and is concentration dependent (~ d 1.7-2.0). We have not been able to discern the origin of the 2:1 integration of these two peaks, though the total integration of the two singlets is ~3, consistent with our assignment to the methyl protons. We suspect that the singlets are due to methyl association with a heteroatom, given their high chemical shifts, and have tentatively assigned them as methoxide protons. ^{13}C NMR of the same solution accounts for 10 carbon peaks, consistent with the ^{1}H NMR, one peak being located upfield at d 55.6. Elemental analysis suggests the molecular formula is $C_{21}H_{23}N_4O_7OsRe$. Expected for this molecular weight: C, 30.76; H, 2.83; N, 6.83; O, 13.66; Os, 23.20; Re, 22.71. Found for the sample: C, 30.54; H, 2.28; N, 6.90 and duplicate C, 30.00; H, 2.49; N, 6.80. Based on this combined evidence we have proposed the structure seen in Figure S2 without implication of the orientation of the ligands around the Re fragment. We believe the oxygen based ligands are planar, given the symmetry of the pyridyl peaks in the NMR spectra.

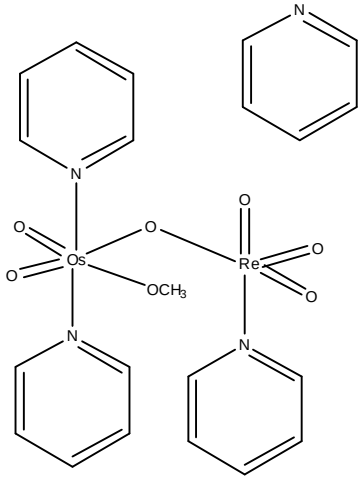

Figure S2. Proposed structure for product of reaction between MTO and OsO_4 in neat pyridine.

Attempts, by several methods, to obtain crystals from this material suitable for X-ray diffraction studies have failed, though they are ongoing and will be presented if successful.

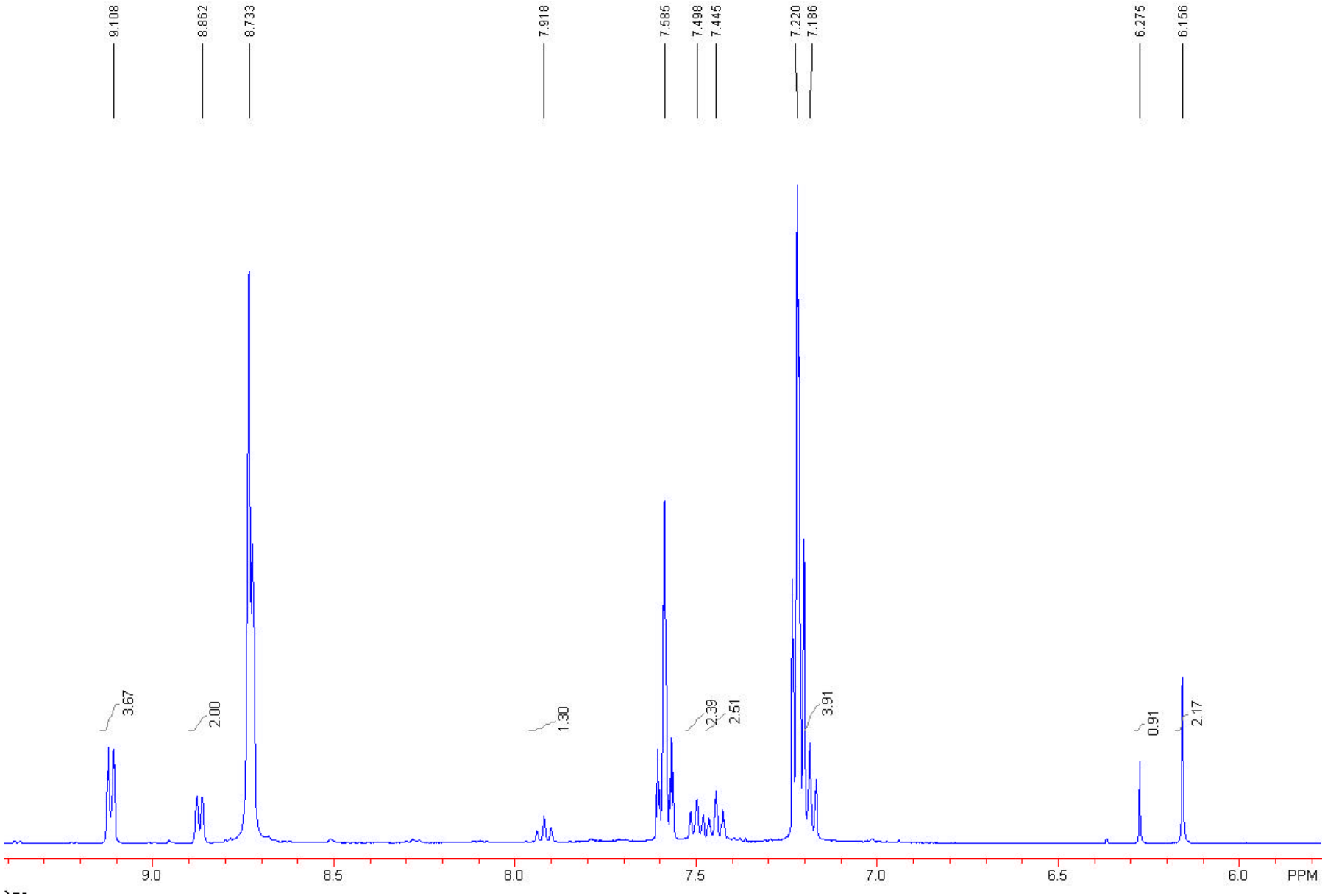

Figure S3. 400 MHz ^{1}H NMR (aromatic region) of reaction product from MTO + OsO_4 in neat pyridine dissolved in py-*d5*.

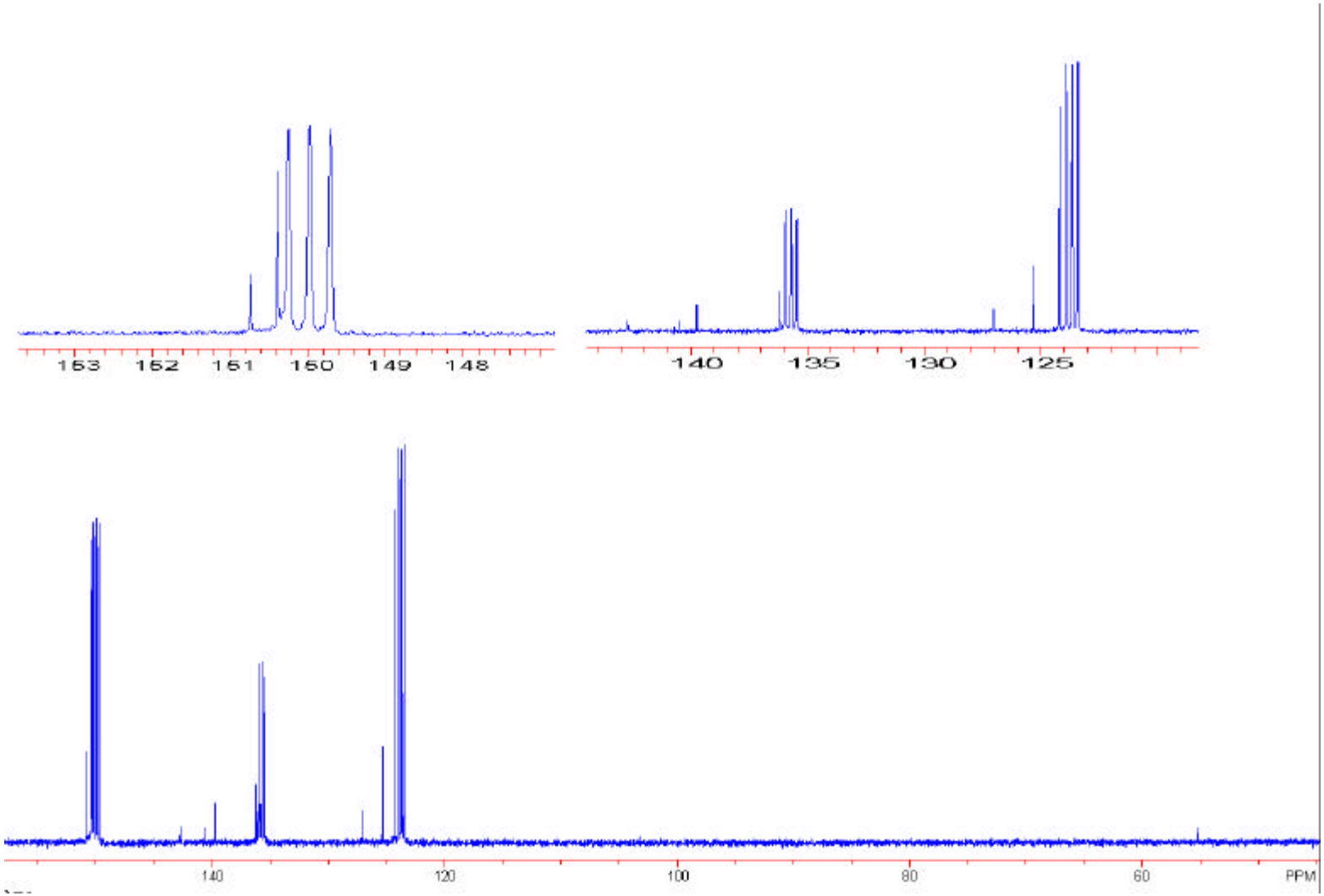

Figure S4. 400 MHz ^{13}C NMR of reaction product from MTO + OsO_4 in neat pyridine dissolved in py-*d5*.

Computational Methods:

The following includes the geometric structures (in Angstroms) and solution phase enthalpies (in kcal mol^{-1}) for the necessary reactants, transition states and products. In addition to the species mentioned in the communication additional reaction pathways of higher enthalpy are included.

Quantum mechanical computations were performed using the B3LYP density functional. This functional is a combination of the hybrid three-parameter Becke exchange functional (B3)[2] and the Lee-Yang-Parr correlation functional (LYP).[3] The basis sets used with B3LYP were constructed as follows. For rhenium we used the core-valence effective core potential of Hay and Wadt,[4] while the Pople-style 6-31G** basis set[5] was utilized for hydrogen, carbon and oxygen atoms. Since some reactions include negatively charged species, the effects of diffuse functions were included by computing single point energies with the 6-11G**++ basis set.[6,7] The combination of the ECP and basis set is referred to as LACVP** or LACVP**++.

All calculations were corrected for the effect of solvent interactions by using the polarizable continuum model (PCM) of solvation.[8,9] We solvated with water, with a dielectric constant of 80.37 and a probe radius of 1.40 Å. The final enthalpy was computed as:

$$H = E_{SCF}^{GP} + E_{ZPVE}^{GP} + E_{tr}^{GP} + E_{rot}^{GP} + E_{vib}^{GP} + E_{solv}$$

Where E_{SCF}^{GP} is the B3LYP/LACVP**++//B3LYP/LACVP energy. For hydroxide the solvation energy used was the experimental value of -102.90 kcal mol^{-1} measured by Tissandier et al.[10]

Below are the computed equilibrium of Re and Os oxo anions.

$OsO_4 + OH^- \rightarrow [OsO_4(OH)]^- \Delta H = -1.5$ kcal mol^{-1} (S1)

$[OsO_4(OH)]^- + OH^- \rightarrow [OsO_5]^{2-} + H_2O \Delta H = -3.9$ kcal mol^{-1} (S2)

$CH_3ReO_3 + OH^- \rightarrow [CH_3ReO_3(OH)]^- \Delta H = -6.4$ kcal mol^{-1} (S3)

$CH_3ReO_3(OH)^- + OH^- \rightarrow [CH_3ReO_4]^{2-} + H_2O \Delta H = -3.4$ kcal mol^{-1} (S4)

Figure S5 shows the important frontier orbitals and their interactions in the TSs for the reaction pathways of Figure 4 in the manuscript. For the low energy (2+3) pathway, the HOMO of $CH_3ReO_4^{2-}$ interacts with the LUMO+1 orbital on the Os bound oxygen through a s -interaction as well as through a p-interaction of the Re-O lone pair with an unoccupied d-orbital on osmium. In the alternative, much higher energy (3+2) TS of OsO_4OH + $MeReO_3OH$, the orbital interactions involve two s -interactions.

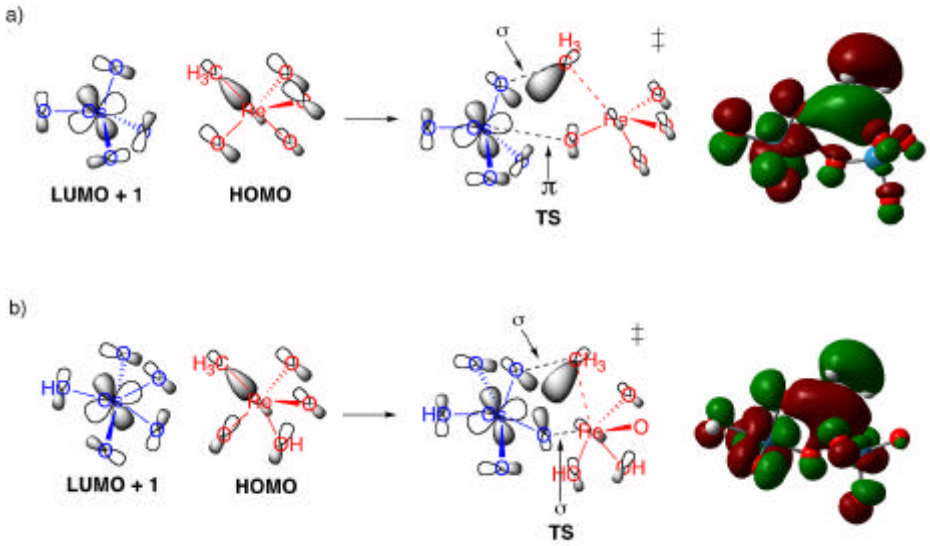

Figure S5. FMO and TS orbital interactions.

1. OH^-

Enthalpy: -75.955491

O	0.7302746777	-0.2280123124	0.3812787519
H	1.1010653770	0.5330398984	-0.1218484279

2. H_2O

Enthalpy: -76.420422

H	.0000000000	.0000000000	.0000000000
O	.0000000000	.0000000000	.9649402977
H	.9364263498	.0000000000	1.1977829378

3. OsO4

Enthalpy: -391.930337

O	0.0580513741	-0.0799777376	2.0275567689
O	-0.3111609038	-0.4946330240	4.7692073023
O	2.1303871511	-1.1537146471	3.5714106973
O	-0.1498148848	-2.6815580210	3.0320616728
Os	0.4322595916	-1.1022648261	3.3503172382

4. $OsO_4(OH)^-$ axial OH

Enthalpy: -467.888104

Os	-0.7469096428	0.5576507081	0.0173290251
O	-0.7637114383	1.2980769646	-1.5538190199
O	-0.4928462051	1.6854137375	1.3397633142
O	1.3326161226	0.6068129092	0.0163285283
O	-2.4789825822	0.4045639619	0.2902956412
O	-0.4101600155	-1.1508304982	-0.0123632053
H	1.5480623797	1.4302391906	0.4733945980

5. $OsO_4(OH)^-$ equatorial OH

Enthalpy: -467.885892

Os	-.5469180388	.5511094912	.0411472503
O	-.7461968755	1.4020750110	-1.7705257399
O	-.4711852344	1.4217645354	1.5469552965
O	1.1473198077	.8255045493	-.4641704353
O	-2.2956643442	.6173811250	-.1891451525
O	-.4117008387	-1.1595733285	.3363458895
H	.1901774621	1.5317960446	-2.0015749951

6. CH_3ReO_3 (MTO)

Enthalpy: -344.734004

Re	0.0226800516	-0.0393152074	0.9840731779
O	-0.0420342788	0.0746283099	-0.7182474158
O	-0.8669297413	-1.3548667404	1.6113574231
O	1.6062793176	0.0731071735	1.6127014857
C	-0.9608811120	1.6639885884	1.6791620604
H	-0.4362739067	2.5475384299	1.3061421460
H	-0.9522639110	1.6521171554	2.7722114888
H	-1.9892317515	1.6500741802	1.3086276706

7. $CH_3ReO_3(OH)^-$ [MTO(OH)-]

Enthalpy: -420.699546

Re	-0.0292208236	-0.2162078937	0.8576259078
O	-0.5650016695	0.2905160171	-0.7034612170
O	-1.2476939032	-1.1326762065	1.6677200516
O	1.4596893519	0.6950373633	1.8326014643
C	-0.8339974559	1.6501175340	1.7467557955
H	-0.3017462138	2.5157820319	1.3486719137
H	-0.7291330038	1.6243924955	2.8327981832
H	-1.8928170607	1.6953969513	1.4690707956
O	1.3006224177	-1.3449648800	0.5632872773
H	2.1932662709	0.0767911007	1.6727549365

8. $CH_3ReO_4^{2-}$

Enthalpy: -420.239992

Re	-0.0489822155	0.0070068445	1.1814958263
O	0.5793680322	-1.5990114835	1.5639232620
C	1.6449742034	-0.0954105786	-0.4701513158
H	1.4673799738	-0.9421885561	-1.1574914156
H	2.6385271891	-0.2289390338	-0.0053818870
H	1.6636546797	0.8350750296	-1.0658457516
O	-1.3350719649	0.0848463100	2.4300080290
O	0.8920460393	1.4092972930	1.6982429395
O	-1.0730273979	0.1787213242	-0.2472744594

9. Lower energy(3+2) Transition State from Communication

Enthalpy: -812.154083

Os	-0.6342148082	-0.3314518377	0.0880564161
O	0.9368706730	0.5435817591	1.6479416676
Re	2.5801734366	0.4736898765	2.2984154502
C	1.9412747123	-2.3750024600	2.2379696183
O	0.3772667847	-1.7391003159	0.3403825921
O	-1.6900231369	0.0123422080	1.4379855794
O	0.1114030905	0.8854382672	-0.9192598366
O	-1.8220665878	-0.9824432096	-1.0534552270
H	2.2408303796	-2.8661154361	1.3193254331
H	2.6955284627	-2.3263009415	3.0195846377
H	0.9332464671	-2.5911994668	2.5770304081
O	2.6731936541	-0.0487601442	3.9579984272
O	3.8080420742	-0.2430966611	1.2994611657
O	3.0287602833	2.1603986242	2.3683541570

10. Higher energy(3+2) Transition State from Communication

Enthalpy: -888.555638

Os	-0.4801458766	-0.1982250200	0.1672924683
O	0.4958648986	0.4062532482	1.6186132612
Re	2.4950467826	0.3455165976	2.4032224787
C	1.5962647925	-2.2278732301	2.2313405581
O	0.2861380278	-1.7738557514	0.2578389176
O	-2.0280077519	-0.1094757724	0.9660788780
O	0.2364753868	0.8627283441	-1.0205022605
O	-1.6767156132	-0.7969018965	-1.4582619798
H	1.9624251411	-2.8333907709	1.4114376771
H	2.3030734830	-2.1223619941	3.0525801657
H	0.5850150370	-2.4414740557	2.5562238234
O	3.8099015260	-0.2369398051	3.3760275169
O	1.2914131585	0.1081219566	4.0014034989
O	3.0403926653	-0.0519893525	0.8022147669
O	2.6309027225	2.0755385904	2.4522948801
H	0.3988058796	0.1330729581	3.6282535091
H	-1.1006618414	-0.6069735660	-2.2103860265

11. Baeyer-Villiger Transition State from Communication

Enthalpy: -888.545938

Re	-0.1167620527	-0.0228849788	-0.0603929754
O	-0.3687069981	-0.2557126016	1.9076668165
C	1.7119228979	-0.2333244377	1.7797417888
Os	-1.4239344052	-0.3497881589	3.5938543425
O	0.5773162276	1.5931785526	-0.0196340015
O	-1.8686626682	-0.0065966524	-0.1739293112
O	0.5839065448	-1.5848649077	-0.4061681291
H	1.7042735208	-1.2173894395	2.2334482686
H	1.6875467230	0.6115004549	2.4578923964
H	2.3992486758	-0.1246705032	0.9406295316
O	-0.6118485420	1.0884029795	4.1651524309
O	-0.7288121205	-1.9165885542	3.9245601147
O	-2.7133234981	-0.3966727493	4.8289561788
O	-2.9658467879	-0.1769847892	2.4094436612
H	-2.6230860590	-0.1191588512	1.4915153243
O	0.0733603083	0.2185255855	-2.0890184818
H	0.0483128224	1.1800545988	-2.1867393985

12. (3+2) Product from Communication

Enthalpy: -888.655941

Os	-0.8131302459	1.4760611305	-0.5990818831
O	-1.0195240422	3.2043873985	-0.3262679341
O	1.0365435959	1.7557217531	0.2998743977
O	-2.6604597745	1.2881438207	-1.1770285617
O	-1.4039310821	0.3233840586	0.8402809820
H	1.2349837636	2.6823850767	0.0987165973
O	-0.0844489782	0.6780525239	-1.9503082761
C	-0.5609807403	-0.0490442870	1.9101355060
H	-1.1389918146	0.0251532615	2.8441944879
H	-0.2407040293	-1.0981374578	1.7914280153
H	0.3262661659	0.5903038670	1.9619390142
Re	-4.1912957866	0.3886114577	-0.2531714584
O	-4.8308116134	-0.1930696264	1.2568306997
O	-5.5574935549	0.7391801527	-1.2640402962
O	-3.5679812663	-1.1104946069	-0.8949207299
O	-4.0013148942	2.1465703977	0.7218135491
H	-3.3521296524	2.6696105231	0.2276236381

13. Baeyer-Villiger Product A from Communication: $OsO_3(OH)^-$

Enthalpy: -392.707503

O	0.7217205546	0.0546634884	1.9002344620
O	-0.3093444848	-0.1359127073	4.6413204859
O	2.3363064999	-0.9177805009	3.2692783407
O	-0.2481085010	-2.5438302316	2.8604687118
Os	0.4245352784	-1.0267602446	3.3517005574
H	2.3543513146	-0.3211197570	2.4632586882

14. Baeyer-Villiger Product B from Communication: CH_3-O-$ReO_3(OH)^-$

Enthalpy: -495.980999

Re	-.0080395503	.3977583442	.7909653909
O	.7644183454	2.2268421557	.5736506222
O	.1323060733	.4016879462	2.5220197054
O	1.3779070065	-.2770628727	-.0306185151
O	-1.4502484180	.9830193860	.0320183720
O	-.8551250230	-1.4109803465	.7965589021
C	-.1064223977	-2.4827100153	1.2773070312
H	-.6734675239	-3.4192149691	1.1549198585
H	.8525928273	-2.5768533441	.7359057949
H	.1368513770	-2.3613779294	2.3496957341
H	1.7195184072	2.1689725111	.7080700347

15. Higher Enthalpy (3+2) Transition State (Connects to 12)

Enthalpy: -888.553605

Os	-0.1348301123	-0.0310607493	-0.0115264668
O	-0.1444047095	0.0645527247	1.7485801071
C	2.0091002548	0.0071276218	2.8616675530
Re	2.9729650960	-1.8162959382	1.1073393748
O	1.6426474646	-0.5467479599	-0.0129810982
O	-2.0929831470	0.6839621927	0.1108980844
O	0.1625206488	1.4252977229	-0.9323152524
H	3.0146150297	-0.2787366786	3.1652237231
H	1.9347590686	1.0321461867	2.5186984849
H	1.2346399643	-0.3116072521	3.5488788728
O	1.5696818325	-2.6824468621	1.6547092868
O	3.4542181838	-2.6976081546	-0.3103858978
O	4.1457782384	-2.2398662304	2.3151696408
O	-0.7812221741	-1.4906323800	-0.6981441623
H	-2.2874512342	0.5551875451	1.0482176164
O	4.0244352128	-0.1339254742	0.7513164306
H	3.4145109146	0.4198422905	0.2432336566

16. Higher Enthalpy (3+2) Transition State (Connects to 18)

Enthalpy: -888.547570

Os	-0.2785171412	-0.2767355453	-0.0728094969
O	0.4241188676	0.2890197032	1.5258850405
Re	2.3081159217	0.3571541419	2.5895125123
C	1.9592109320	-2.3247310277	1.8494105581
O	0.7207327706	-1.7563347416	-0.0296414279
O	-1.3772649041	1.4904733097	0.0621099277
O	0.3370896524	0.3228219399	-1.5892732329
O	-1.8187287045	-1.1042051222	0.0080551218
H	-0.9676763030	1.9138975389	0.8277026808
H	2.5237102233	-2.6628512433	0.9908283385
H	2.5552591887	-2.1858173150	2.7507268071
H	1.0160754287	-2.8275633091	2.0238963274
O	3.5820350071	-0.1812889907	3.6364872645
O	0.9759857930	-0.3692967816	3.8971694789
O	3.0830370306	0.3328295201	1.0365740917
O	2.1334974358	2.0478625696	2.9328638690
H	0.1570069615	-0.4561245566	3.3890306620

17. Higher Energy (3+2) Transition State (Connects to 12)

Enthalpy: -888.545569

Os	-0.1298328369	0.2034382544	0.1187032475
O	0.0477449213	0.2494259830	1.8686309779
C	2.1284361652	0.1479996136	2.9049545173
Re	2.8088001312	-1.9097032202	0.9481070788
O	1.6710128326	-0.4318500549	0.0476915175
O	-1.9087682131	0.0238496920	0.1063207409
O	0.0939605577	1.8032692040	-0.5196438250
H	3.1308802853	-0.2636647446	2.9936435544
H	2.0967964807	1.1897245515	2.6087966305
H	1.4367474798	-0.1464001272	3.6855814001
O	1.3258377960	-2.5635656773	1.5771641474
O	3.0918586295	-2.8586101017	-0.4809644407
O	3.9592476524	-2.4662495514	2.1267444282
O	-0.3188288324	-1.2706492145	-1.1990217153
O	4.0828658526	-0.3859959877	0.5889505747
H	3.5174034439	0.2788784301	0.1692068978
H	0.6000855342	-1.5672272100	-1.3106630557

18. Alternative (3+2) Product

Enthalpy: -888.669349

Os	-0.9511692321	1.7758568098	-0.5351425447
O	-1.0082468894	3.3954763432	0.1056904333
O	0.2532327742	0.5101551924	-0.4332357728
O	-2.5629388078	1.2620413826	-1.3753847396
O	-1.9389342331	0.9700990905	1.0798887543
O	-0.2722000914	2.3761197952	-2.3232479384
C	-1.2770461084	0.2382132563	2.0630925679
H	-0.7482646698	0.9001753202	2.7764377704
H	-2.0140356794	-0.3542926599	2.6248278347
H	-0.5294518361	-0.4392241093	1.6168010911
Re	-3.8974971696	0.1050479490	-0.1716234324
O	-4.5701216305	-0.3427310631	1.3662208605
O	-5.1339994179	-0.2231137799	-1.3416169062
O	-2.7752847597	-1.1960339875	-0.4560730444
O	-4.4305589188	2.0035100418	0.1874186858
H	-3.8326527526	2.5576584569	-0.3312331883
H	-1.0376157839	2.1523323713	-2.8762739375

19. $[CH_3ReO_3(OH)]^-$ Decomposition TS

Re	0.0054357359	-0.0264470180	0.0067094804
O	-0.0114053154	-0.0712122972	1.7325340259
O	1.6031878017	-0.2482639060	-0.6092011073
O	-1.0722628785	1.2327315998	-0.8594784704
C	0.8303494109	2.4699854267	0.4856879950
H	0.3587455582	2.9168387385	1.3709905120
H	1.0721710530	3.2742466380	-0.2291958591
H	1.7893705393	2.0439250488	0.7983923254
O	-0.8550644245	-1.4430033170	-0.4740183355
H	-0.3663186488	1.9698065492	-0.3944475326

(1) Conley, B.L.; Ganesh, S.K.; Gonzales, J.M.; Tenn, W.J., III; Young, K.J.H.; Oxgaard, J.; Goddard, W.A., III; Periana, R.A. *J. Am. Chem. Soc.* **2006,** *128,* 9018.

(2) Becke, A. D., *J. Chem. Phys.* **1993,** 98, 5648.

(3) Lee, C.; Yang, W.; Parr, R. G., *Phys. Rev. B.* **1988,** 37, 785.

(4) Hay, P. J.; Wadt, W. R., *J. Chem. Phys.* **1985,** 82, 299.

(5) Hariharan, P. C.; Pople, J. A., *Theo. Chim. Acta.* **1973,** 28, 213.

(6) Krishnan, R.; Binkley, J. S.; Seeger, R.; Pople, J. A., *J. Chem. Phys.* **1980,** 72, 650.

(7) Clark, T.; Chandrasekhar, J.; Schleyer, P. v. R., *J. Comput. Chem.* **1983,** 4, 294.

(8) Tannor, D. J.; Marten, B.; Murphy, R.; Friesner, R. A.; Sitkoff, D.; Nicholls, A.; Ringnalda, M.; Goddard, W. A.; Honig, B., *J. Am. Chem. Soc.* **1994,** 116, 11775.

(9) Martin, J. M. L., *Chem. Phys. Lett.* **1996,** 259, 669.

(10) Tissandier, M. D.; Cowen, K. A.; Feng, W. Y.; Gundlach, E.; Cohen, M. H.; Earheart, A. D.; Coe, J. V.; Tuttle, T. R., *J. Phys. Chem. A* **1998,** 102, 7787.